

SYNCHRONIZING AND STABILIZATION OF WEAK GRIDS WITH VSC AND NONLINEAR POWER DAMPING CONTROL

R. Jaya shubha¹, K. Shabana banu²

^{1,2}Student, Department of EEE, JNTUA, Anantapuramu, Andhra Pradesh, India

Abstract- *This paper presents a new methodology for a weak grid is to make possible the addition of voltage source converters more effective. The controller is mainly composed of two parts, namely linear power damping and synchronizing controller and a supplementary nonlinear controller. The first part synchronizes a voltage source converter (VSC) to the grid by supplying damping and synchronizing power components automatically and injects full power under very weak grid conditions. The frequency and angle regulation of the linear controller are chosen from the cascaded angle, frequency and power loops. In spite of stable and smooth operation of linear controller in various cases, the stability of the weak grids cannot be guaranteed under sudden large transients which quickly transfers system dynamics to nonlinear region. In order to succeed this problem, the second part i.e the supplementary nonlinear controller is designed along with the linear controller to intensify the performance of the system under certain large disturbances such as low power and high power injection, self-synchronization and fault-ride-through conditions in weak grids. Simulation results of the proposed controller were carried out in MATLAB/SIMULINK environment. Simulation results prove that the proposed nonlinear controller improves the performance of the system under abnormal disturbances and shows the effective working of the controller. By replacing the dc source of the controller with a photovoltaic system, improved profiles are obtained and the cost of operation of the entire system is reduced than before which are to be observed from the simulation results of the replaced controller.*

Key Words: Distributed generation, nonlinear control, power damping, voltage source converter (VSC) control, weak grid.

1. INTRODUCTION

The Environmental friendly renewable energy technologies such as wind and solar energy systems are among the fleet of new generating technologies driving the demand for distributed generation of electricity [1]. Based on renewable energy sources such as solar power,

wind power, small hydro power etc. The distributed generation systems encounter the increment in the power demand. The major driving force in the context of smart grids is smooth combination of DG units. For interfacing the renewable and clean energy assets, VSCs are the primary empowering technology in modern grids. Vector control[2] and direct power control[5] are the main controlling techniques of VSCs. In order to determine the grid angle and initial angle, the PLL are required which assure the seamless converter grid connection through the process of synchronization[6]. During abnormal changes, the PLL motion harmfully attacks the entire system stability in weak grids. In spite of the advantages, there is a lot of leaning towards developing new control techniques which exclude the use of PLL [7]. To overcome the troubles injected with vector control of VSCs connected to weak grids, the concept of power synchronization [8] has been introduced to supply an essential synchronization with grid in steady state which mimics a synchronous generator. The proposed methods are developed based on small signal dynamics and cannot assure huge-signal security.

Actually, the measure of uniting line ability to transfer power to the grid depends on the grid firmness i.e., the weak ac grids face more problems for power flow transfer and the available power transfer is confined [10]. The short-circuit capacity ratio (SCR) is suggested as a pointer of an ac system strength compared to the power rating of a VSC, which indicates the strength of ac systems. The downside of the vector control is its confined capacity to exchange rated power in weak grids. In whatever way, the developed methods for weak grid combination are depended on linearized models and fail to offer the self-synchronization and attachment and play operation.

Besides, islanded operation of DG units can be permitted to improve service reliability [9]. Power organizing in detached operation of VSCs is frequency hang down [10], which is most regular approach which causes a fixed frequency offset. In this way when self-synchronization is applied, frequency and angle mismatch between a VSC and a grid at the point of integration may cause severe sudden changes. In addition, major concern related to VSC operation in

weak grids is the deficiency of physical inactivity in routine VSCs, a poor overall frequency and load angle regulation. Therefore, separated operation of microgrids with high entrance of VSCs can be disposed to frequency instability. As needed, important endeavors has been shortly devoted to introduce some dynamics for frequency using virtual inactivity. As a rule, the virtual inactivity eludes a short term energy preservation which is integrated to a VSC [11], the virtual inactivity is equated by proper dc-link control [12].

Stimulated by the above call to respond, a hybrid nonlinear controller of VSCs in powerless networks is proposed in this paper.

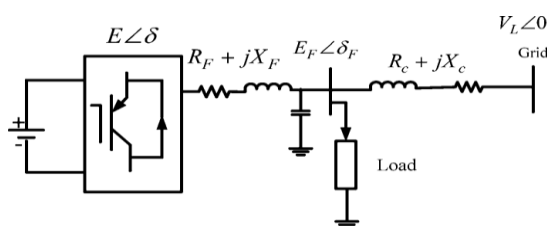


Fig-1: Circuit diagram of a grid-connected VSC.

The controller receives a force synchronization loop with extra cascaded damping and synchronizing loop. The important qualities of the proposed controller are brief accounted as follows:

- The hybrid nonlinear power damping controller switch on self-synchronization of a VSC in powerless grids. This implies that the controller does not require a additional synchronization unit and it spontaneously synchronizes itself with the grid. Self-synchronization is a new idea[7] and its imperativeness is more heard in powerless grids. It ought to be noted that the technique still needs the commencement time of synchronization and some data from the isolated grid, thus it cannot realize a true plug and play operation. Additionally, its reliability and stability in powerless grids have not been examined. It is intimated that during seperation, an MG may normally aquire fixed frequency drop indicating reliable frequency and angle mismatch at the point of reconnection. Nevertheless, the proposed controller system does not use any beginning synchronization with grid and it uses a plug and play system.
- The controller consists of cascaded frequency, angle and power loops. As a result, great degree of stability edge and oscillating qualities can be obtained. In this paper, the issue is explained by using a frequency loop as primary controller. Accordingly, the frequency

reference is probably set equated to the grid nominal frequency.

- Because the controller has a dynamic way of acting which resemble conventional SGs. It can be connected to very weak grids with SCR=1 without stability loss.
- To assure system security in all working conditions in particular when load angle jumps to nonlinear area, a nonlinear supplementary controller is determined.
- The controller is appropriate to both modes of working i.e separated mode and matrix connected mode. Accordingly, the requirement for islanding identification and system reconfiguration are removed simultaneously.
- It supplies fault-ride-through capability by accurate fitting of frequency, load angle and voltage sufficiency, which in turn results in limiting current passing into the interacting network.

The proposed control topology is regular as it is operatively connected to a VSC-based high voltage dc (HVDC) transmission systems.

2. PROPOSED LINEAR CONTROLLER TOPOLOGY

This paper concentrates on the concept of introducing a nonlinear power damping control strategy for VSC units in weak grids which are applicable to both grid connected and islanded modes of operation.

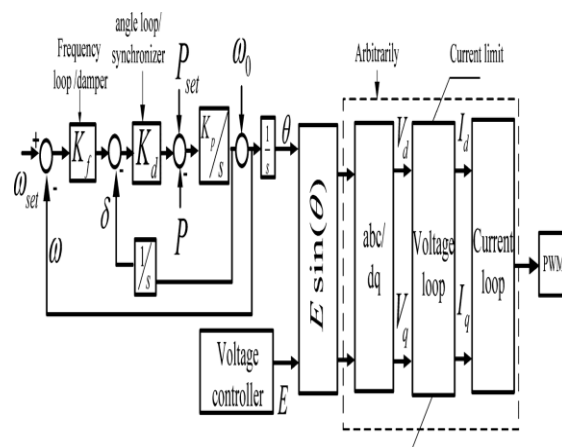


Fig-2: Proposed linear control scheme.

Fig .1 shows the diagrammatic view of a grid-connected VSC supplying a local load. The complexity of the system due to nonlinear character of the power transfer dynamics is the most serious issue for controller design. Generally, linear controllers are designed based on small-signal linearization. However, the controller performance essentially depends on particular operating points. A two-level topology with interactive nonlinear and linear controllers are developed in this paper. The first stage is a power synchronizing-damping controller. The second stage is a nonlinear controller which strengthen the linear controller to intensify system stability in powerless gridsor during self-synchronization where the load angle is more and the system operates under nonlinear region. The voltage generation principle mimic to an SG where the voltage frequency and load angle are adjusted by force damping-synchronizing loop, taking into consideration the voltage amplitude is given by voltage regulation loop which mimic to an automatic voltage regulator (AVR). The VSCs output power real power is verified directly by assessing the load angle using the power-oscillating loop, in contrast the reactive power is verified by assessing the volatge size. Since the VSC is the voltage-controlled one, an inbuilt current loop is not required which exclude during big sudden changes such as errors where the control should be moved to current control case to fix the current abundance[8]. It should be stated that the suggested outer-loop controller can be also added with cascaded voltage-current loops to get high power quality drive and essential current margins during disturbances. In this aspect, the synchronization angle for dq-reference frame conversion is acquired from the introduced controller in place of PLL as represented in fig.2.

2.1 Power synchronization control concept

The principle of power damping control concept of a grid-connected VSC is that the controller furnish active damping and synchronization power to reduce power,frequency and load angle fluctuations and synchronize VSC with the grid during steady state operation. Fig .2 describes the fundamental principle of the proposed controller which mainly contains three loops that is frequency,angle and power loops. The reference of the load angle is obtained based on the frequency error. The real power reference is determined as a function of the load angle error. Finally, the power synchronization loop adjusts VSCs frequency and load angle. The synchronization and the damping power components which are obtained from angle and frequency loops essentially find the divergance of the grid and spontaneously synchronizes itself with the grid. When the main source falls short to supply the fixed power, short-term energy accumilate can be joined to the dc-link to counterbalance for the energy requirement

during sudden changes. The counterbalanced real power is given by

$$P = \frac{E}{R^2 + X^2} (XV_L \sin\delta + R(E - V_L \cos\delta)) \dots\dots(1)$$

The above equation states that the real power that can be emitted from a VSC is margined. The SCR is described to determine the capacity of the associated line.

$$SCR = \frac{\text{short circuit capacity}}{\text{rated dc power}} \dots\dots(2)$$

The short-circuit capacity of the ac system is expressed as

$$S_{SC} = \frac{E_0^2}{Z} \dots\dots(3)$$

And Z is the equivalent Thevenin's impedance.

The power damping control law for a VSC is proposed as

$$\frac{d\Delta w}{dt} = -K_p K_f K_d (w - w_{set}) - K_p K_f \delta - K_p (P - P_{set}) \dots\dots(4)$$

To get rid of the switching effect superimposed on real power, a low-pass filter can be added and purified power is passed to the controller.

The damping and the synchronizing power components are expressed as

$$\Delta P_{damp} = -K_f K_d \Delta w \dots\dots(5)$$

$$\Delta P_{synch} = -K_d \Delta w \dots\dots(6)$$

The above two powers weakens load angle and frequency disturbances across an equilibrium point and synchronize the VSC with the grid. Because of the inbuilt frequency and angle loops of the VSCs, the use of the PLL in steady-state operation and under several transient conditions is eliminated.

2.2 Voltage amplitude controller

The reactive power of the DG unit can be controlled to

- To control the fatal voltage.
- Obtain exact output reactive power.

In the P-V bus control, the voltage reference is compared with the existing output voltage. A proportional-integral (PI) controller is added intended at counter balancing the input deviation by suitable adjustment of VSCs output voltage which is used to trace the reference voltage.

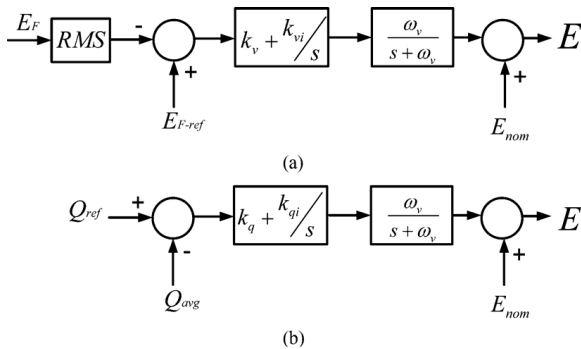


Fig-3:control topologies for output voltage control. (a) P-V bus control. (b) P-Q bus control strategy.

The output of the PI controller is progressed by a low-pass filter and lastly the VSCs voltage amplitude reference is determined. Generally, it is required to regulate the grid-voltage at the point of common coupling in powerless grids. Therefore, P-V bus is the general approach in weak grids.

Another choice of the voltage control is reactive power regulation as shown in fig.3(b). In whatever way, this is not the common case because the P-Q control strategy indicatively reduces DG stability in weak grids when referred to P-V control. The working of the P-Q bus control strategy is similar to that of P-V bus control strategy.

3.SYSTEM MODELING

A detailed study of small-signal stability of a grid-connected VSC is explained here in order to assess the system dynamic behaviour in a powerless grid. The three-phase power system mainly contains a converter and its controller, RL filter, transmission line and infinite grid. Considering VSC as ideal, the controller order is evenly balanced by the VSC local load voltage. Therefore, it is capable of modeling the VSC and PWM block by an average voltage approach[13]. The parameters of the system are presented in Table 1. The obtained model of the VSC and its controller can be obtained as follows. The load angle dynamic equation is represented by

$$\Delta \dot{\delta} = \Delta \omega \dots \dots (7)$$

The frequency dynamic expression is given by (4) where ΔP is given by

$$\Delta P = \frac{\partial p}{\partial \delta} \Delta \delta + \frac{\partial p}{\partial E_F} \Delta E_F \dots \dots (8)$$

Table -1: Controller parameters

Parameter	Value (SI units)
VSC maximum power capacity	7MW
VSC voltage(L-L rms)	4160v
E_{f-ref} (phase maximum voltage)	3400v
K_f	5
K_d	1e5
K_p	0.1
K_v	200
K_{vi}	100
ω_v	500

The voltage loop dynamic expression is given by

$$\Delta \dot{E} = -w_v \Delta E + w_v \Delta v - w_v K_v \Delta E_F \dots \dots (9)$$

$$\Delta \dot{v} = -K_{vi} \Delta E_F \dots \dots (10)$$

Where v represents output of the integrator K_{vi} , E_F is the filter voltage amplitude represented by

$$\Delta E_F = \frac{E_{Fd0} \Delta E_{Fd} + E_{Fq0} \Delta E_{Fq}}{E_{F0}} \dots \dots (11)$$

$$\Delta E_{Fd} = L_c \frac{d \Delta i_d}{dt} + R_c \Delta i_d - w_0 L_c \Delta i_q \dots \dots (12)$$

$$\Delta E_{Fq} = L_c \frac{d \Delta i_q}{dt} + R_c \Delta i_q + w_0 L_c \Delta i_d \dots \dots (13)$$

The current dynamics in the dq reference-frame are given by

$$\frac{d \Delta i_d}{dt} = \frac{1}{L} (-E_0 \sin \delta_0 \Delta \delta + \Delta E \cos \delta_0 - R \Delta i_d + w_0 L \Delta i_q) \dots \dots (14)$$

$$\frac{d \Delta i_q}{dt} = \frac{1}{L} (E_0 \cos \delta_0 \Delta \delta + \Delta E \sin \delta_0 - R \Delta i_q - w_0 L \Delta i_d) \dots \dots (15)$$

Expressions (4) and (7)-(15) represent a sixth order system and contain all the eigen values of the multivariable multi-input multi-output controller and the connected power system. At the time of design process, even though small values of K_f and larger magnitudes of $\frac{K_{vi}}{K_v}$ yields a high stability margin and quick response, the steady-state error is abnormally incremented particularly in weak grids with high load angle. Therefore, load angle oscillations becomes more at the point of instability during contingencies.

4.NONLINEAR POWER DAMPING CONTROLLER

A nonlinear back-stepping power damping controller is designed and added to the linear controller to overcome the problem of weak performance and instability which is as shown in Fig.4.

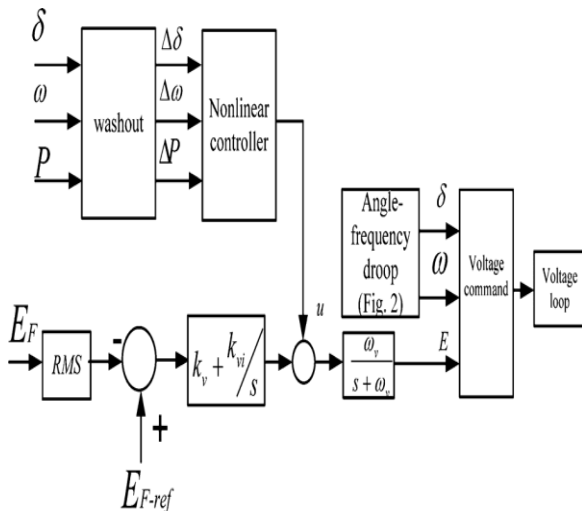


Fig-4: Nonlinear supplementary control structure.

The entire system model is

$$\dot{x}_1 = x_2 \quad \dots \dots (16)$$

$$\dot{x}_2 = a_1 x_1 + a_2 x_2 + a_3 x_3 \quad \dots \dots (17)$$

$$\dot{x}_3 = u_f + E \frac{V_L}{X} x_2 \cos x_1 - w_v x_3 \quad \dots \dots (18)$$

Where $a_1 = -K_p K_d$, $a_2 = -K_p K_d K_f$ and $a_3 = -K_p$ and $[x_1, x_2, x_3] = [\Delta\delta, \Delta\omega, \Delta P]$. u_f is described by $u_f = (u_w V_L \sin x_1) / X$, where u is the control input. The aim is to confirm the deviation of the error $e_i = x_i - x_{i,ref}$ to 0. The initial step is to make δ stabilised, thus the Lyapunov function

$$V_1 = \frac{1}{2} x_1^2 \quad \dots \dots (19)$$

Is defined and the reference of the frequency deviation value and V_1 are given by

$$x_{2ref} = -k_1 x_1 \quad k_1 > 0 \quad \dots \dots (20)$$

$$\dot{v}_1 = -k_1 x_1^2 + x_1 e_2 \quad \dots \dots (21)$$

In the following step, the lyapunov function is defined as $V_2 = V_1 + 1/2 e_2^2$ and x_{3ref} is selected to stabilize V_1 and V_2 .

Where

$$c_1 = \frac{(1 - k_1(-a_2 + k_1) + a_1)}{a_3} \quad \dots \dots (23)$$

$$c_2 = -\frac{(k_1 + k_2 + a_2)}{a_3} \quad k_2 > 0 \quad \dots \dots (24)$$

Lastly, by describing

$$V_3 = V_2 + \frac{1}{2} e_3^2 \quad \dots \dots (25)$$

The entire system stability is confirmed when

$$u_f = \left(A + k_1 \frac{EV_L}{X} \cos x_1 \right) x_1 + \left(B - \frac{EV_L}{X} \cos x_1 - a_3 \right) e_2 + (C - k_2)$$

Where

$$A = K_f - k_1^2 K_f + k_1 K_d K_f - 2k_1 K_p + \frac{k_1^3}{K_p} - \frac{k_2}{K_p} \quad (27)$$

$$B = (k_1 + k_2 - K_d) K_f + \frac{1 - k_1^2 - k_2^2 - k_1 k_2}{K_p} \quad (28)$$

$$C = -k_1 - k_2 + K_p K_f \quad \dots \dots (29)$$

And the simplified form is

$$V_3 = -k_1 x_1^2 - k_2 e_2^2 - k_3 e_3^2 \quad \dots \dots (30)$$

The structures of the controllers are decoupled because the nonlinear controller is additional one which supplies an added signal for the linear controller.

5. PHOTOVOLTAIC SYSTEM

Solar photovoltaic system is fundamentally used for grid-connected electricity to function for lighting and air conditioning, residential appliances, commercial equipment for all types of buildings. To meet any stage of power requirements, solar PV units can be made into a group as an array of series and parallel joined units. Technical barriers are not found while interconnecting PV system to local utility company which is easy based on technical aspect. Exactly speaking, group working of solar panels, the visible part of the PV system, and does not add all other hardware which include in a solar array.

5.1 Photovoltaic array

In order to obtain higher voltages, currents and power levels, photovoltaic cells are joined electrically in series and/or parallel circuits. The primary building blocks of PV systems are the photovoltaic units consisting of PV cell circuits enclosed in an environmentally protective lamination. One or more PV units are gathered as a pre-wired, field installable unit which includes photo voltaic panels combined to form a photovoltaic array which is a complete power generating unit.

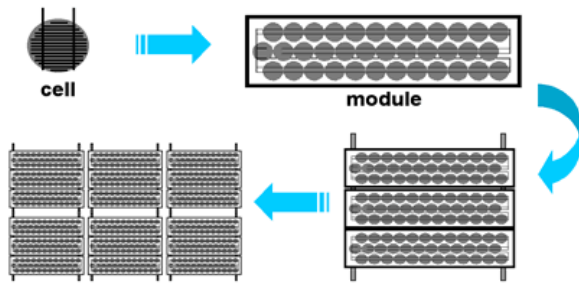


Fig-5: photovoltaic cells,modules,panels and arrays

According to the maximum Dc power output which is obtained from the functioning of pv modules and arrays, under standard test conditions (STC) which are highly safe and reliable.

Auxiliary energy sources, battery bank, a DC-AC power inverter, system and battery controller and sometimes the specified electrical load (appliances) are the components of the major photovoltaic system.

Presently, distinctive advantages such as absence of fuel cost, simplicity of assigning, high dependability, no noise, wear and tear is less due to absence of moving parts and low maintenance which increases the importance of PV generation , assuming as a RES application. In addition, the solar energy describes a pollution free, inexhaustible and clean energy source. The ascending reliability of solar cells, decreasing prices and cost of solar units and manufacturing technology improvements are the additional factors. The increasing importances of cost reduction of certain PV converters are obtained from the regular declining prices of the PV modules.

6.EVALUATION RESULTS

The arrangement of the simulated system is as shown in fig 5. The system consists of a 7.0MW VSC, filter ,local load ,trasformer and a bridge line connecting the VSC to the grid . having a specific value to indicate that the impedance 0.2+j0.5Ω is the equivalent impedance of the strong source referring to the spreading(distribution) level.the simulation of the system is carried out in MATLAB/SIMULINK platform.

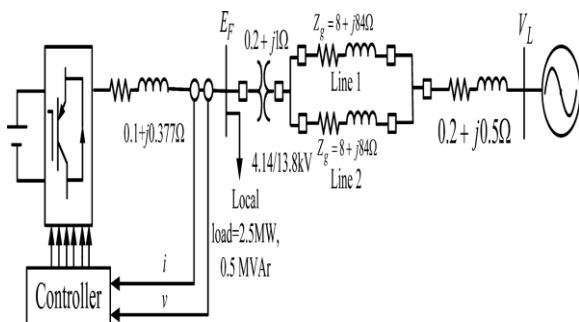


Fig-6: Simulated system.

The paramrters of the controller are represented in the table 1. The local load at the output terminal is provided by the DG unit and it is joined to a strong grid by means of a very lacking strength interface with total impedance of $|Z|=|R+jX|=|4.4+j43.5|=43.7\Omega$. during this period , the connecting line is very nearly inductive, the power capacity of the interface line is proximated by

$$P \approx \frac{E_F V_L}{X} \sin \delta_F \dots\dots(31)$$

Where notations are explained in fig 1.and X is total reactance of the transformer,line and strong grid . therefore, the maximum real power trasfer capacity of the joining the line is equal to $P_{max}=13880^2/43.5\sim 4.44MW$

During the connection of the grid , the DG acts as a PV bus intended at maintaing the filter output voltage as fixed quantity. To determine the accurateness of the proposed hybrid nonlinear controller, a different variety of postulated sequences are tested. The performance of the system is evaluated by considering different modes such as low and high power injections, transition to islanding mode, sudden deviation in grid angle, self-synchronisation and three phase disturbances. Flexibility to work in various operating conditions is the main advantage of proposed controller. The following results can be obtained from the simulation designs.

6.1 Low-power injection

A distance range of operating points are to be studied to determine the behaviour of the controller. It is to be imagined that, at the starting system supplies 80KW, and $t=1s$, the reference power is incremented to 2.0MW, the response of real power is shown in fig.7, which views a seamless transition. The rise time is about 0.6s and perfect reference record without any overshoot.

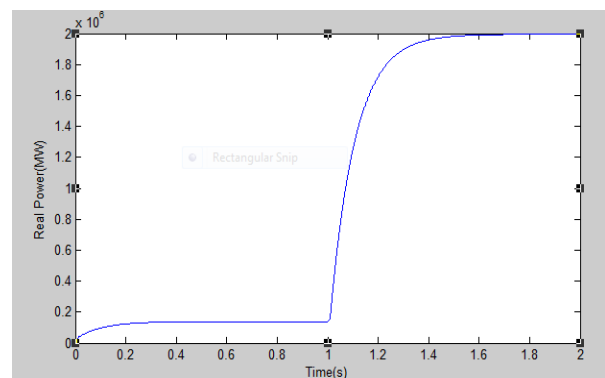


Fig-7:Controller performance in low-power injection.

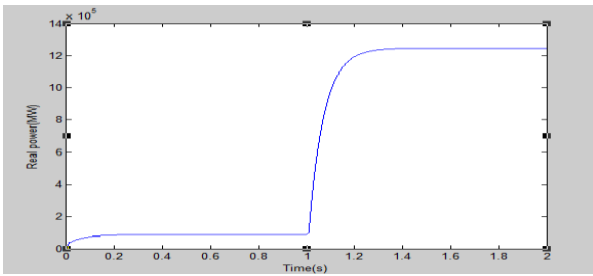


Fig-8:Controller performance in low-power injection when replaced by pv system.

6.2 High-power injection

The reference power is changed to 2.0MW to 6.0MW indicating closeness to the VSCs maximum power capacity at fixed voltage working and a load angle more than 1.03 rad is expected. Fig 9 depicts the real power and output phase voltage variation waveforms as shown. It is to be noted that the response is smooth but contains a greater rise-time. The output phase voltage amplitude presents the controller performance to encourage VSCs voltage at the time of load angle variation to provide high real power injection. The general characteristics of the system which gives rise to voltage sag subsequent to increase in output power and at the same time with high voltage drop, which is a contrast.

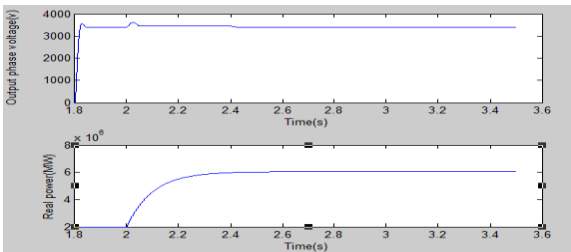


Fig-9:Real power and phase-voltage amplitude in high-power injection.

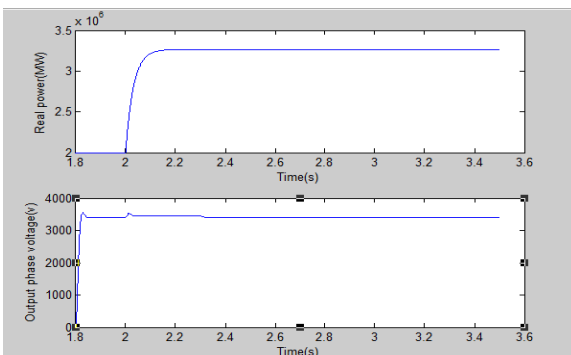


Fig-10:Real power and phase-voltage amplitude in high-power injection when replaced by pv system.

6.3 Transition to island mode

The another postulated sequence that may exist in DG applications to supply local critical loads is islanded operation. At $t=4s$ the VSC is jumped to the separated mode because of fault in the grid. Reconfiguration of the system is not needed. Fig 11 shows the smooth transition without any unstable factors. Large steady state deviations in the grid connected mode are attained when K_f is decremented to obtain quick response. The respective current waveforms are observed which are smooth and fast transition because of the majority of the controller in either modes of operation.

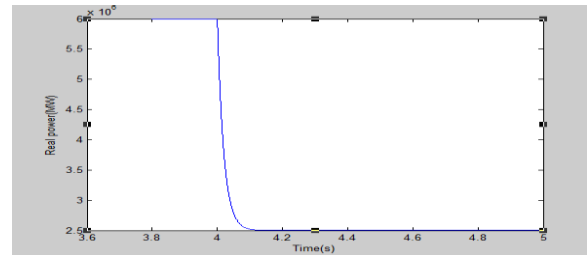


Fig-11:Real power during transition to islanding.

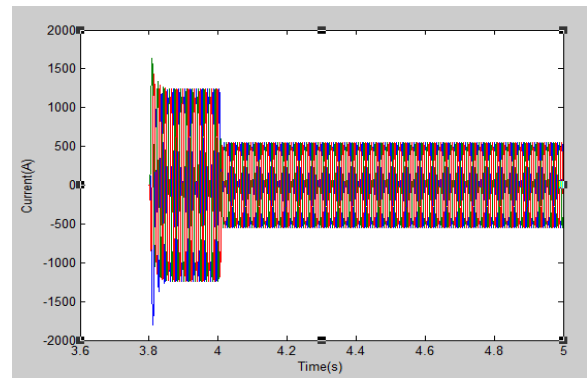


Fig-12:Current waveforms subsequent to islanding.

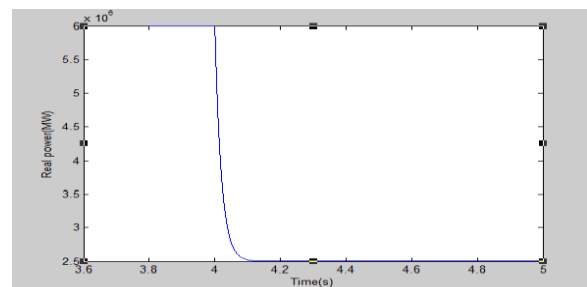


Fig-13:Real power during transition to islanding when replaced by pv system.

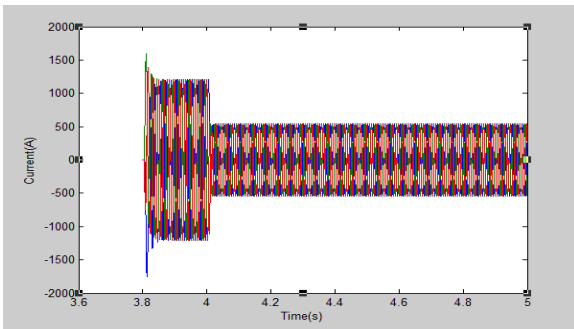
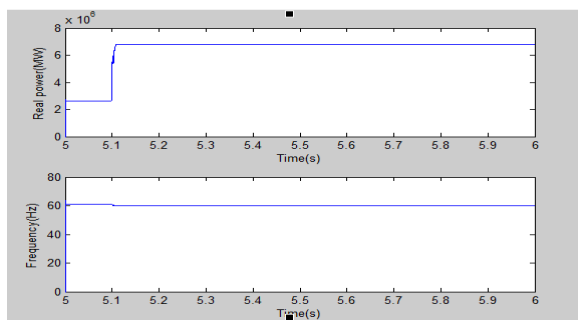


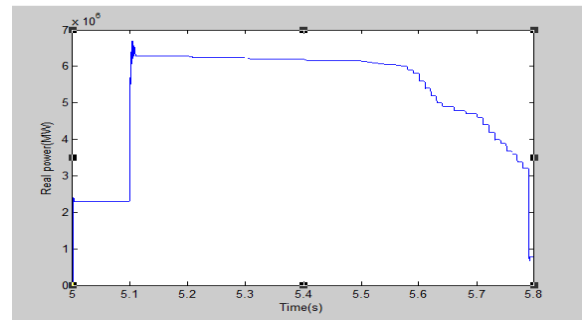
Fig-14:Current waveforms subsequent to islanding when replaced by pv system.

6.4 Self-synchronized grid restoration

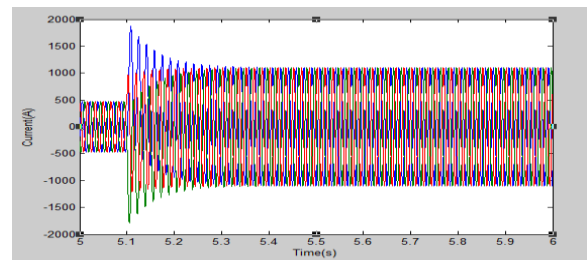
In general, spontaneous recloser again reconnects a DG unit to the source grid after a specified time period. Numerous faults are vanished after few cycles, which is the general truth. In this case connection occurs without synchronization leading to heavy transients which are resulted from the mismatch of angle and frequency on both sides during connection at that point of time. Powerless grids have more transients during resynchronization because of the fact that load angle is essentially large and after grid restoration moves to the nonlinear region freely. Fig 15(a) shows the respective waveforms and depicts that the system with nonlinear controller supplies smooth and quick grid connection. The system response without using the supplementary controller is depicted in fig 15(b), shows that powerless grid connections cause instability. Fig 15(c) shows the current waveform of the system with supplementary controller depicts the well-damped characteristics even in the out-of-phase reclosing modes.



(a)

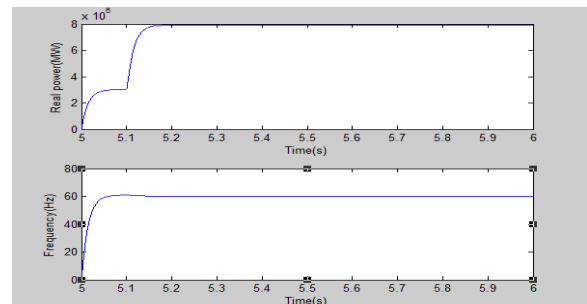


(b)

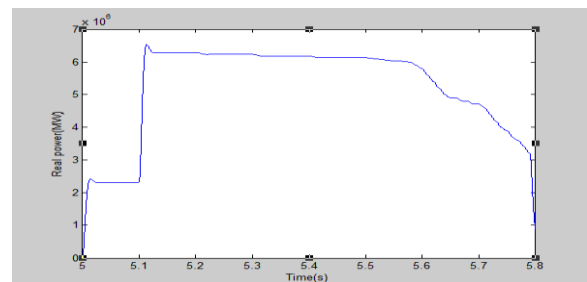


(c)

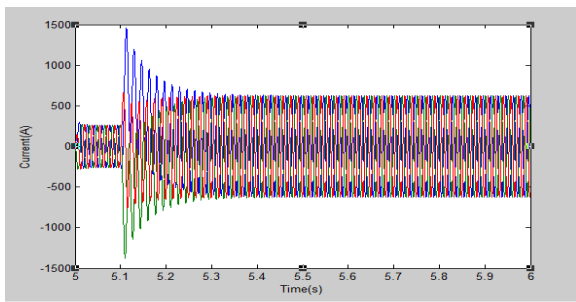
Fig-15:System performance during grid restoration. (a) Real power and frequency with nonlinear supplementary controller. (b)Real power without the supplementary controller. (c) Current waveforms subsequent to self-synchronization with supplementary controller.



(a)



(b)



(c)

Fig-16:System performance during grid restoration when replaced by pv system. (a) Real power and frequency with nonlinear supplementary controller. (b)Real power without the supplementary controller. (c) Current waveforms subsequent to self-synchronization with supplementary controller.

6.5 Fault-ride-through capability: disturbance in the grid angle

Along with the large connecting impedance, powerless grids may be effected by the sudden changes in the voltage angle and frequency. Fig 17 shows the resulting waveforms of the load angle and phase voltage amplitude respectively,verifies that VSC easily identifies the angle variations even under high disturbances without loss of stability and reduced performance. This is a very interesting quality of the controller where it works as a virtual PLL, and automatically monitors grid frequency and angle deviations. If we observe the waveforms in Fig 17, we can justify that the output voltage amplitude is drastically decremented to keep the output power limited. The fact behind that is decrement in the grid voltage angle exhibits sudden increase in output power. Therefore, the output voltage must be decreased to maintain real power stability.

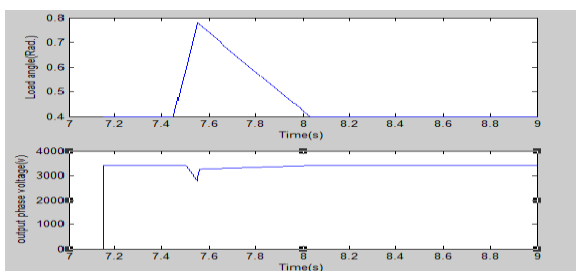


Fig-17:Load angle and output phase voltage variation subsequent to disturbance in grid angle.

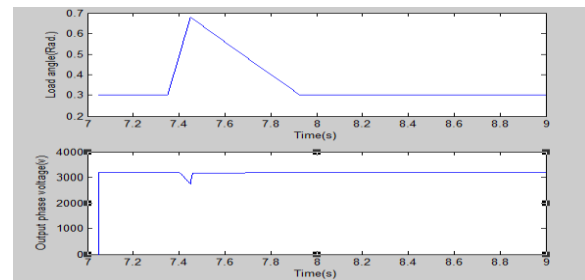


Fig-18:Load angle and output phase voltage variation subsequent to disturbance in grid angle when replaced by pv system.

6.6 Fault-ride-through capability: Three-phase fault

Fig.19 visualize the VSC’s fault-ride-through execution when a three-phase bolted fault strikes near to the end of connecting line 2. The fault is initiated at $t = 9s$ and the line 2 is seperated from the grid by the guard system after 0.16s. fig.19 views the waveforms of the output real power, current and phase voltage amplitude. From the waveforms , it is known that VSC is not subjected to over-currents duing three-phase faults. At the event of fault, the real power waveform is seamless and restricted, the voltage drops and the reactive power is incremented. At $t = 9s$, the circuit breakers on bothsides of the connecting line 2 becomes active and the line is seperated from rest of the grid. Large signal changes occurs in the system during the isolation of the connecting line. After the separation of the line 2 at $t = 9s$, voltage,real power and current replaces back to the initial conditions before the fault but the operating points are different. This verifies the uncertainties of the system during the sudden large transients. The reconnection of the connecting line 2 is smooth and the waveforms presents well-damped charecteristics which can be observed.

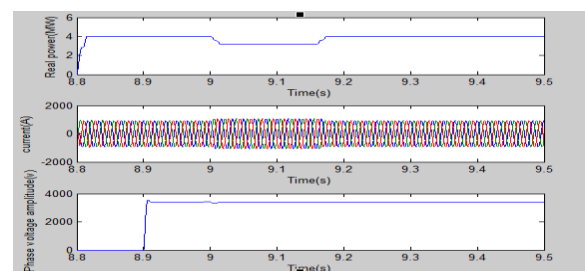


Fig-19:Real power, Instantaneous current and Phase-voltage amplitude subsequent to a three-phase fault.

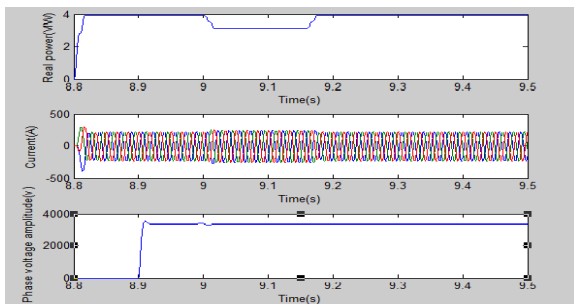


Fig-20:Real power, Instantaneous current and Phase-voltage amplitude subsequent to a three-phase fault when replaced by pv system.

If it is assumed that if the fault is cleared at $t = 10.16s$ when line 2 is again switched into the circuit. The waveform corresponding to the reconnection of line 2 such as real power, current, amplitude of the phase voltage and load angle are as shown in ig.21. When the line 2 is activated after the reclosure, the overall system settles down in 0.7s. The reconnection of connecting line 2 is smooth and all the waveforms present well-damped characteristics.

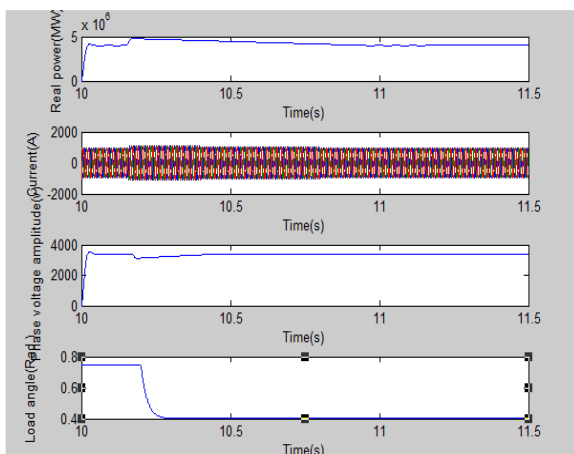


Fig-21:Real power, Instantaneous current, output phase voltage and load angle subsequent to reconnecton of line 2.

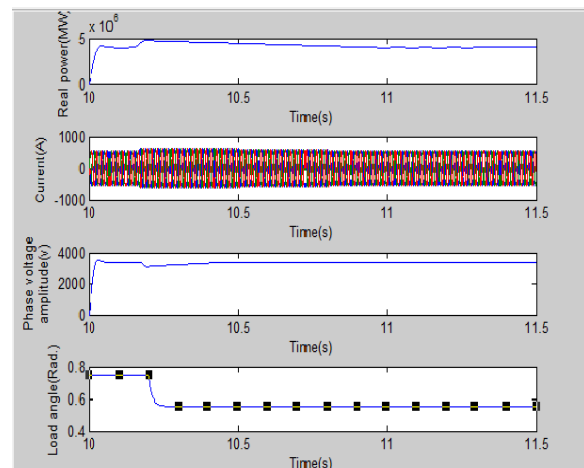


Fig-22:Real power, Instantaneous current, output phase voltage and load angle subsequent to reconnecton of line 2 when replaced by pv system.

7. Conclusion

In this paper, a new control methology weak grids is presented which is to make possible the addition of voltage converters more effective. The controller consists of two parts which are the linear power damping controller and the nonlinear supplementary controller. The linear part resembles SGS along with additional power damping-synchronization capacity supplying self-synchronization with grid which vanishes rhe use of a PLL. If the VSC and grid ferequency and angle match incorrectly during grid replacing scenarios which results in weak perrformance and instability. Large-signal transients are considered ins this case. In order to improve the system performance in these cases the proposed nonlinear controller is used. In addition, the controller is capable of working in very weak grids $SCR < 2$ and submits rated power for the reason of having damping and synchronizing power components. To determine the validation and accurateness of the controller, the linear and nonlinear parts are designed and has been presented in various simulation scenarios. When the dc source of the system are replaced by a photovoltaic system, improved profiles are obtained and the cost of operation of the entire system is reduced than before. Grid-connected PV systems can provide a number of benefits to electric utilities, such as power loss reduction, improvement in the voltage profile, and reduction in the maintenance and operational costs of the electric network. Advanced inverter, controller, and interconnection technology development must produce hardware that allows PV to operate safely with the utility and act as a grid resource that provides benefits to both the grid and the owner. Advanced PV system technologies include inverters, controllers, related balance-of-system, and energy

management hardware that are necessary to ensure safe and optimized integrations.

By comparing the total harmonic distortion values of the current in various modes of operation of the controller, we can observe that the distortion is reduced as shown in the table.

Table -2: Comparision of percentage of THD

Mode of operation	% of THD when connected to a dc source	% of THD when Connected to a PV system
Islanding	66.36%	54.65%
self-synchronization with supplementary control	42.51%	35.07%
Three-phase fault	22.30%	14.45%
Reconnection of line 2	40.30%	25.50%

References

[1] A. Guerrero *et al.*, "Distributed generation," *IEEE Ind. Electron. Mag.*, pp. 52–64, Mar. 2010.

[2] N. Flourentzou, V. G. Agelidis, and G. D. Demetriades, "VSC-based HVDC power transmission systems: An overview," *IEEE Trans. Power Electron.*, vol. 24, no. 3, pp. 592–602, Mar. 2009.

[3] B. Parkhideh and S. Bhattacharya, "Vector-controlled voltage-source converter-based transmission under grid disturbances," *IEEE Trans. Power Electron.*, vol. 28, no. 2, pp. 661–672, 2012.

[4] Y.-P. Ding and J.-H. Liu, "Study on vector control used in VSC-HVDC," in *Proc. IEEE Power Engineering and Automation Conf. (PEAM)*, 2011.

[5] J. Verwecken, F. Silva, D. Barros, and J. Driesen, "Direct power control of series converter of unified power-flowcontroller with three-level neutral point clamped converter," *IEEE Trans. Power Del.*, vol. 27, no.4, pp. 1772–1782, Oct. 2012.

[6] F. Blaabjerg, R. Teodorescu, M. Liserre, and A. V. Timbus, "Overview of control and grid synchronization for distributed power generation systems," *IEEE Trans. Ind. Electron.*, vol. 53, no. 5, pp. 1398–1408, Oct. 2006.

[7] Q. -C. Zhong, P. -L. Nguyen, Z. Ma, and W. Sheng, "Self-synchronised synchronverters: inverters

without a dedicated synchronization unit," *IEEE Trans. Power Electron.*, vol. 29, no. 2, pp. 617–630, 2014.

[8] L. Zhang, L. Harnefors, and H.-P. Nee, "Interconnection of two very weak ac systems by VSC-HVDC links using power-synchronization control," *IEEE Trans. Power Syst.*, vol. 26, no. 1, pp. 344–355, Feb. 2011.

[9] "Ieee guide for design, operation, and integration of distributed resource island systems with electric power systems," *IEEE Std. 1547.4-2011*, pp. 1–54, Jul. 2011.

[10] K. Vischer and S. W. H. D. Haan, "Virtual synchronous machines (VSG's) for frequency stabilization in future grids with a significant share of decentralized generation," in *Proc. IET. CIRED, Smart Grid for Distribution*, 2008.

[11] M. F. M. Arani and E. F. El-Saadani, "Implementing virtual inertia in DFIG-based wind power generation," *IEEE Trans. Power Syst.*, vol.28, no. 2, pp. 1373–1384, May 2013.

[12] J. Zhu, C. D. Booth, G. P. Adam, A. J. Roscoe, and C. G. Bright, "Inertia emulation control strategy for VSC-HVDC transmission systems," *IEEE Trans. Power Syst.*, vol. 28, no. 2, pp. 1277–1287, May 2013.

[13] G. Weiss, Q. -C. Zhong, T. C. Green, and J. Liang, "Repetitive control of DC-AC converters in microgrids," *IEEE Trans. Power Electron.*, vol. 1, no. 1, pp. 219–224, Jan. 2004.

[14] S. M. Ashabani and Y. A. -R. I. Mohamed, "A flexible control strategy for grid-connected and islanded microgrids with enhanced stability using nonlinear microgrid stabilizer," *IEEE Trans. Smart Grid*, vol. 3, no. 3, pp. 1291–1301, Sep. 2012.

BIOGRAPHIES

R. Jaya Shubha has received the B.Tech degree from K.S.R.M College of engineering, Kadapa in the stream of electrical and electronics engineering in 2013 and presently persuing M.Tech at JNTUA College of engineering, Anantapuramu.

K. Shabana Banu has received the B.Tech degree from J.N.T.U Pulivendula in the stream of electrical and electronics engineering in 2013 and presently persuing M.Tech at JNTUA College of engineering, Anantapuramu.















